Response modification factor
of suspended zipper braced frames

Gholamreza Abdollahzadeh [*1] and Mehdi Abbasi [2a]

[1] *Faculty of Civil Engineering, Babol University of Technology, Babol, Iran*
[2] *Civil Engineering Department, Shomal University, Amol, Iran*

Abstract. The suspended zipper bracing system is suggested to reduce the flaws of ordinary zipper braced and concentric inverted *V* braced frames. In the design procedure of suspended zipper bracing systems, columns and top story truss elements are strengthened. This bracing system show different performances and characteristics compared with inverted *V* braced and ordinary zipper frames. As a result, a different response modification factor for suspend zipper frames is needed. In this research paper, the response modification factor of suspended zipper frames was obtained using the incremental dynamic analysis. Suspended zipper braced frames with different stories and bay lengths were selected to be representations of the design space. To analyze the frames, a number of models were constructed and calibrated using experimental data. These archetype models were subjected to 44 earthquake records of the FEMA-P695 project data set. The incremental dynamic analysis and elastic dynamic analysis were carried out to determine the yield base shear value and elastic base shear value of archetype models using the OpenSEES software. The seismic response modification factor for each frame was calculated separately and the values of 9.5 and 13.6 were recommended for ultimate limit state and allowable stress design methods, respectively.

1. Introduction

Given progresses made in applied sciences and experiences gained regarding buildings performances over past earthquakes, seismic engineering and its approach has been profoundly changed. Bracing as the lateral load resistant system is the most common method to resist lateral loads in steel structures. Inverted *V* braced frames due to large lateral stiffness, which decreases inter-story drifts of structures, and their simplicity in design and application are widely used as concentrically braced frames. In these frames, members form a vertical truss that resists lateral loads. This kind of brace suffers from poor energy dissipation and force redistribution capability. Also, as the brace buckles, it produces a large unbalanced vertical load on the intersecting beam because of the emerged difference between compression and tension forces. In order to prevent

---

∗Corresponding author, Associate Professor, E-mail: g.abdollahzadeh@ymail.com

[a] M.Sc. Student

undesirable deterioration of lateral strength, current design provisions require that the beam has adequate strength to resist the post buckling force and gravity loads. This results in very strong beams (Khatib *et al.* 1988). As an alternative to resist this unbalanced load, the proposal of Khatib *et al.* (1988) is to tie all beam-to-brace intersecting points together to make them act simultaneously and carry this unbalanced force to upper stories during an earthquake.

In suspended zipper braced frames, the top story bracing members are designed to remain elastic when the all other compression braces have buckled and all the zipper columns are yielded. This bracing system has more detailed design to resist lateral forces more efficiently (Leon and Yang 2003).

Structures after nonlinearity show significant reserve strength and an energy dissipation capacity. Reserve strength (over-strength) and energy dissipation capacity (i.e., ductility) form a base shear force reduction factor, *R*. Using the *R* concept implies that structures are designed in their elastic range by considering their inelastic performance. ATC-19 (1995) and ATC-34 (1995) propose *R* as a product of over-strength, ductility and redundancy factors. This study evaluates the over-strength force reduction resulted from the ductility and response modification factors of eight zipper braced frames designed in accordance with AISC (2005).

2. Suspended zipper braced frames

Khatib *et al.* (1988) conducted a thorough study on the post buckling characteristics of inverted *V* braced frames. In inverted *V* braced frames subjected to an earthquake, by continued lateral displacement, compression brace buckles and forms a plastic hinge that causes a sudden loss of compression strength, while tension strength remains almost untouched. This change of strength creates an unbalanced vertical force on of the beam intersection resulting in an inter-story drift tendency to concentrate in a single story (Yang and Leon 2003). A cyclic behavior of zipper frames is investigated by Yang *et al.* (2010). To increase the ductility and energy dissipation capability of structures, Goel (1992) and Bruneau *et al.* (1998) introduced special concentrically braced frames. However, the main shortcomings of inverted *V* braced frames including the unbalanced force and localization of damage still remained in these frames. Khatib *et al.* (1988) proposed the application of a zipper column in the beam intersection with braces to carry this unbalanced force to upper stories. The intent was to tie all the brace-to-beam intersection points together to force them act simultaneously and redistribute and dissipate the earthquake energy over the building height. The flaw of this approach is that if the compression brace buckles the zipper column carries this force to upper stories causing a compression force in all the beam-to-brace intersection points and unbalanced forces propagate up in the structure resulting in all compression braces to buckle. Simultaneous brace buckling over the height of a building will result in a more uniform distribution of damage, which is considered as a desirable goal. However, instability and collapse can occur once the full-height zipper mechanism forms, as described by Trembleay and Tirca (2003).

To improve the performance of zipper systems, the suspended zipper bracing system is introduced by Leon and Yang (2003). In suspended zipper braced frames, top truss elements are designed to remain elastic while all other compression braces and zipper columns are yielded (Yang and Leon 2003). This system can prevent full height mechanism and redirect the unbalanced vertical force into the exterior columns. Typical performances and *V*-Δ curves of inverted *V* braced frames, ordinary zipper braced frames and suspended zipper braced frames are

shown in Figs. 1, 2 and 3, respectively. Design of zipper columns also is investigated by Kim (Kim *et al.* 2008).
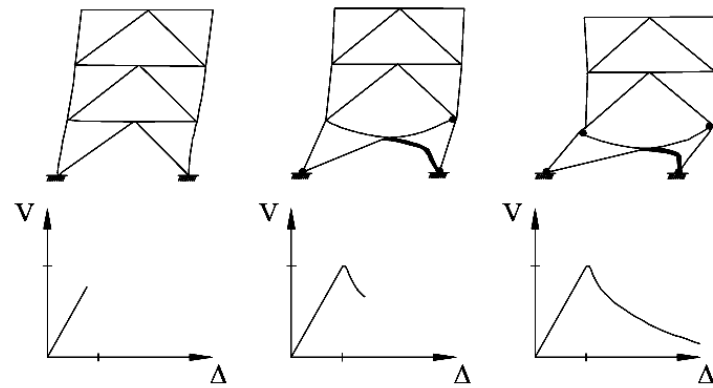

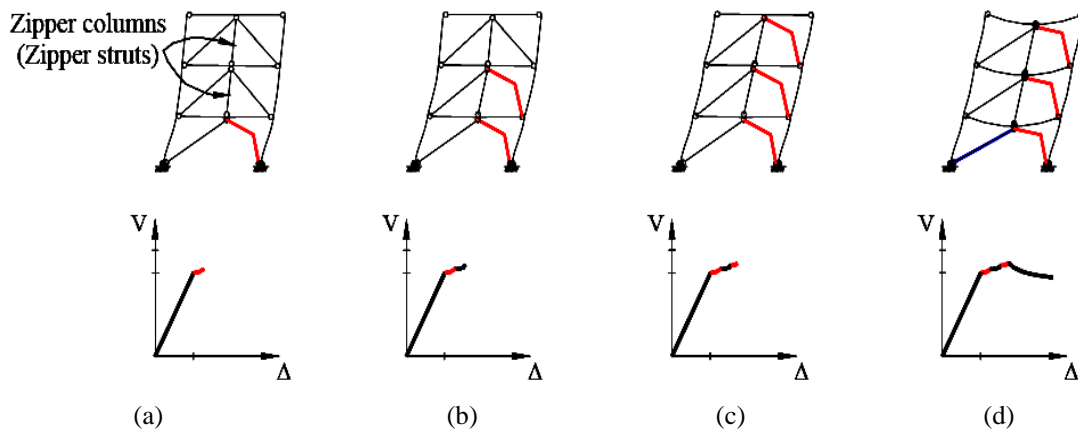Fig. 1 Typical performance and *V*-Δ curve of an inverted *V* braced frame (Yang and Leon 2003)

Fig. 2 Typical performance and *V*-Δ curve of an ordinary zipper braced frame (Yang and Leon 2003)

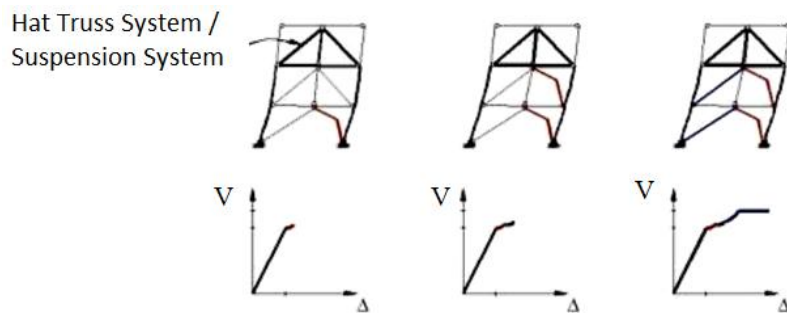Fig. 3 Typical performance and *V*-Δ curve of a suspended zipper braced frame (Yang and Leon 2003)
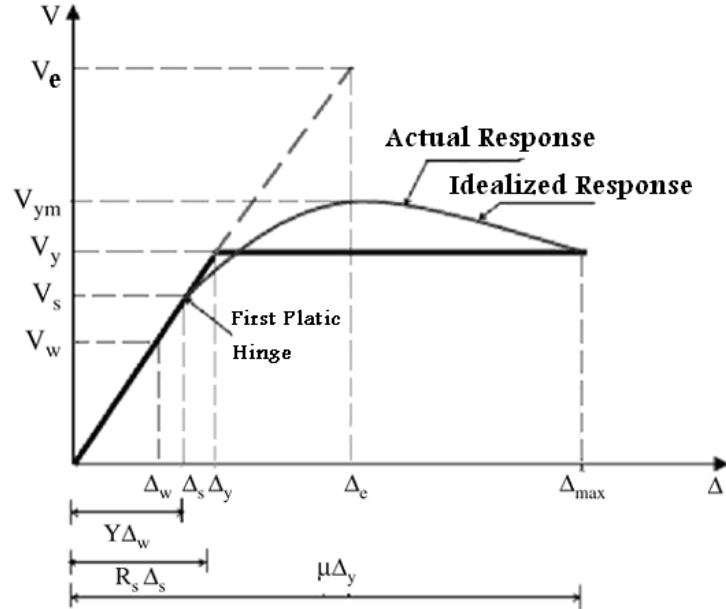
Fig. 4 General structure response (Uang 1991)

3. Response modification factor

The energy dissipation and performance of structures at the time of an earthquake is highly dependent on the nonlinearity of elements. Taking this issue in the design consideration is a very complicated matter and the elastic analysis of structures under the real load of earthquake can result in very big uneconomical sections. To overcome this problem, many seismic codes generally recommend a reduction factor for design loads, taking advantage of the fact that structure has significant reserve strength (overstrength) and the capacity to dissipate energy (ductility) in the inelastic range. Mazzolan and Piluso (1996) addressed some issues in obtaining the response modification factor such as low cycle fatigue and plastic deformation. As shown in Fig. 4, the real nonlinear behavior of structures is usually idealized by a bilinear elastic perfectly plastic relation.

Where *Ve* is elastic response strength, *Vy* is yield response strength of the structure and it is maximum base shear in an elastic- perfectly plastic behavior (Uang 1991). *Vs* is response strength in which first plastic hinge occurs. Force reduction factor, R_μ, is defined as the relation of *Ve* to *Vy*

$$R_\mu = \frac{V_e}{V_y} \tag{1}$$

And over-strength factor is defined as followed

$$R_s = \frac{V_y}{V_s} \tag{2}$$

To calculate actual R_s, other issues must be accounted (Uang 1991).

$$R_s = R_{so} \times F_1 \times F_1 \times \ldots \times F_n \qquad (3)$$

R_{so} is over-strength factor calculated using Eq. (2) which is based on nominal material properties. F_1 is used to account for difference between actual and nominal static strength. The value of F_1 can be taken as 1.05 as proposed by Schmidt and Bartlet (2002). F_2 is the increase factor of yield stress due to the strain rate effect during an earthquake event.

The response modification factor is generally formulated in a way that considers the ductility and over-strength. In order for an ultimate stress design, R is calculated as follows (Uang 1991).

$$R = \frac{V_e}{V_s} = \frac{V_e}{V_y} \times \frac{V_y}{V_s} = R_\mu \times R_s \qquad (4)$$

In order to use the response modification factor in the allowable stress design, codes decrease design loads from Vs to Vw. This is undertaken using the allowable stress factor defined as the ratio of Vs to Vw. In this paper, allowable stress factor, Y, is assumed as 1.44 (Uang 1991).

As such, the response modification factor for the allowable stress design approach is as follows

$$R_w = \frac{V_e}{V_w} = \frac{V_e}{V_y} \times \frac{V_y}{V_s} \times \frac{V_s}{V_w} = R_\mu \times R_s \times Y \qquad (5)$$

Fig. 4 shows an idealized pushover curve for a structure. The push-over analysis is conducted by selecting a lateral load pattern and loading the structure from its initial state to its collapse state. The push-over curve is then carried out by plotting the base shear force versus the lateral displacement of the structure. Because of the simplicity of this curve, it is usually used as an estimation of real performance of structures in real earthquake excitations. However, in reality, excitation scenarios do not follow the selected load pattern and many other factors, namely the fatigue behavior or strain hardening of steel materials, affect the structure performance which is neglected by the pushover analysis. To overcome this, in this research, the pushover curve is estimated via an incremental dynamic analysis using a set of 44 earthquake records. To calculate Vy, the incremental dynamic analysis of each model subjected to the selected earthquakes is carried out. For each model, the first fundamental elastic period is calculated, then records one by one are normalized to their spectral values at the first elastic period, $Sa(T1)$. By scaling new records, using trial and error, $Sa(T1)$ and so peak ground acceleration ,PGA ,of records in which failure happens, is determined. The maximum nonlinear base shear of this time history analysis is Vy (Mwafi and Elnashi 2002). The calculation of Vs was conducted considering that the linear ultimate state of nonlinear static analysis and nonlinear dynamic analysis are the same. The results for determining of zipper response modification factor can be compared with buckling restrained braced frames response modification factor which is obtained by this method by Abdollahzadeh and Banihashemi (2013).

4. Selection of archetype models

To assess the response modification factor, a systematic approach for the characterization of key features related to the seismic resisting system is needed (FEMA-P695 2009). Archetypes are intended to reflect the range of design parameters and system attributes that are judged to be

reasonable representations of the design space and have a measurable impact on the system response (Uang 1991). For braced lateral resisting structures, structural configuration issues affecting the properties of models are the extent of gravity loading tributary to the bracing system, the range of framing span length of braced frames and number of stories. The story height of usual buildings is generally between 10 to 12 feet (3 to 3.6 meters). In this research, the story height is chosen as 11 feet (3.3 meters) as median value of the mentioned range. In the ASCE (2005) document the structure height for bracing the singular lateral resisting system is limited to 160 feet (49 meters). This allows having buildings with 3, 6, 11 and, at most, 15 stories. In this research, braces were designed to sustain 100 percent of the lateral load and beam column joints were assumed to be pinned at both ends. Dead, live and earthquake loads are taken from the ASCE for residential buildings. The AISC (2005) was used to design the bracing frame elements. To take span width and tributary area issues into account, two span widths and bay locations were selected. For the 5-meter bay outer frames and for the 9-meter bay inner frames were selected to place the
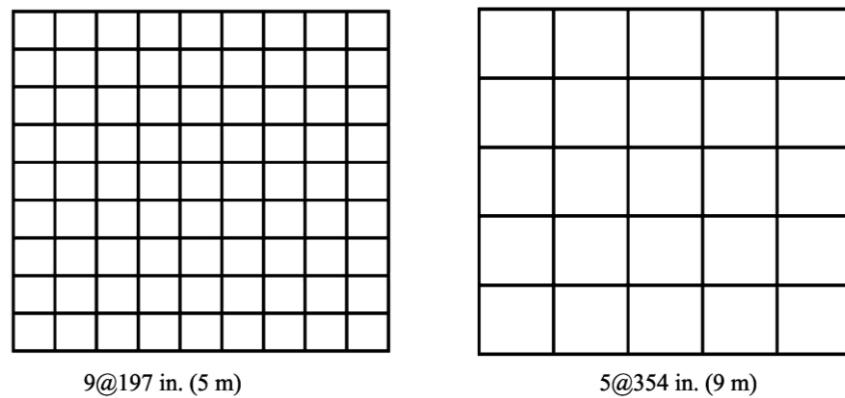

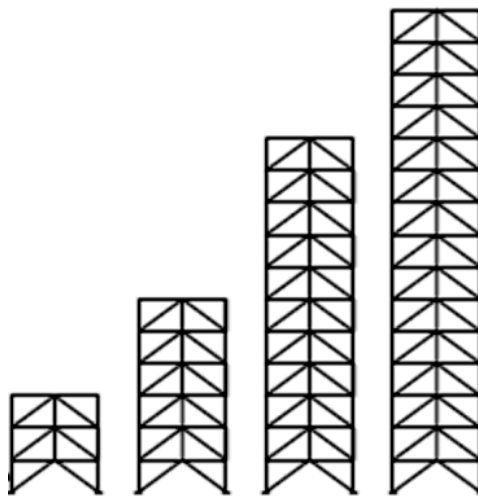Fig. 5 Schematic plan of 9 and 5 meters span width

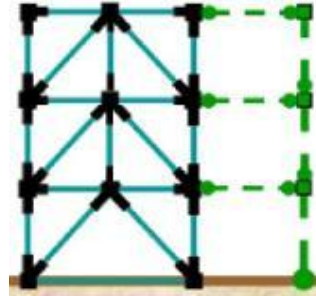Fig. 6 Configuration of braced archetype models

Fig. 7 Sketch of a 3 stories OpenSEES model with dummy column

bracing system. Figs. 8 and 9 show the schematic sketch of archetype models. In 3-, 6- and 11-story buildings there are 6 braced bays in each direction and in the 15-story building there are 8 braced bays in each direction.

Open Systems for Earthquake Engineering Simulation (OpenSEES) was developed by the Pacific Earthquake Engineering Research (PEER) center and used for the analysis. This software is physics based and includes modeling features required for the simulation of braced frame buildings, such as the Uriz fatigue material (Uriz and Mahin 2004), large deformation geometric transformations (Mozzoni 2004), and several numerical algorithms for solving equations associated with nonlinear dynamic and static analyses (Mozzoni 2004). To model the effects of the gravity load, a dummy column was used. In Fig. 10, an OpenSEES model for a braced bay of a 3-story building and its dummy column are shown.

The Fatigue material (Urize 2005) wrapped around the Steel02 material was used to account for strength degradation and low cycle fatigue of steel. The Steel02 material is a Giuffre-Menegotto-Pinto steel material object with isotropic strain hardening (Mozzoni 2004). The fatigue material uses a modified rain flow cycle counting algorithm based on Coffin-Manson log-log relationships to accumulate damage in a material using Miner's Rule (Uriz and Mahin 2004). Element stress-strain relationships become zero when fatigue life is exhausted. Models are named following the span width and number of stories as shown in Table 1. All base supports are assumed as simply supported. Mass of each story is assumed as 359.352 Kips. Initial damping ratio is also assumed as 0.05.

Table 1 First three elastic periods of models

Model ID	Span width (in.)	No. of stories	No. of braced bays	T1 (Sec)	T2 (Sec)	T3 (Sec)
903	354	3	6	0.31	0.10	0.07
906	354	6	6	0.61	0.20	0.11
911	354	11	6	1.05	0.34	018
915	354	15	8	1.65	0.54	0.27
503	197	3	6	0.41	0.13	0.09
506	197	6	6	0.75	0.24	0.12
511	197	11	6	1.32	0.40	0.20
515	197	15	8	2.20	0.62	0.32

5. Model calibration using test data

Uriz (2005) conducted a series of experimental tests on brace elements and used previous experimental studies for calibrating parameters a brace element model in OpenSEES. These experimental results were used in this study to calibrate the analytical model. The parameters calibrated include the number of fiber sections in an element, the number of fibers in a section, rotational spring of connections and fatigue material parameters.

Table 2 Model 903 and 503 frame sections

Model ID	903				503			
Story	Brace	Zipper	Column	Beam	Brace	Zipper	Column	Beam
3	W12×120	W14×61	W12×96	W24×55	W14×82	W12×96	W12×96	W24×55
2	HSS6×6×0.625	W14×43	W12×96	W30×116	HSS6×6×0.375	W12×96	W12×96	W30×90
1	HSS7×7×500	-	W12×96	W24×55	HSS6×6×0.500	-	W12×96	W24×55

Table 3 Model 906 and 506 frame sections

Model ID	906				506			
Story	Brace	Zipper	Column	Beam	Brace	Zipper	Column	Beam
6	W14×233	W14×145	W14×176	W24×55	W14×257	W14×211	W12×96	W24×55
5	HSS7×7×0.500	W14×145	W14×176	W30×211	HSS6×6×0.500	W14×176	W14×193	W30×191
4	HSS8×8×0.500	W14×99	W14×176	W24×55	HSS7×7×0.500	W14×145	W14×211	W24×55
3	HSS8×8×0.500	W14×68	W14×176	W24×55	HSS8×8×0.500	W14×99	W14×211	W24×55
2	HSS8×8×0.625	W14×38	W14×176	W24×55	HSS8×8×0.500	W14×61	W14×233	W24×55
1	HSS8×8×0.625	-	W14×193	W24×55	HSS8×8×0.625	-	W14×233	W24×55

Table 4 Model 911 and 511 frame sections

Model ID	911				511			
Story	Brace	Zipper	Column	Beam	Brace	Zipper	Column	Beam
11	W14×730	W14×426	W14×497	W24×55	W14×665	W14×550	W12×96	W24×55
10	HSS8×8×0.500	W14×370	W14×498	W27×539	HSS6×6×0.500	W14×550	W14×550	W27×539
9	HSS8×8×0.500	W14×370	W14×499	W24×55	HSS8×8×0.500	W14×550	W14×550	W24×55
8	HSS8×8×0.625	W14×342	W14×500	W24×55	HSS8×8×0.625	W14×500	W14×550	W24×55
7	HSS10×10×0.625	W14×311	W14×500	W24×55	HSS8×8×0.625	W14×426	W14×550	W24×55
6	HSS10×10×0.625	W14×257	W14×500	W24×55	HSS10×10×0.625	W14×370	W14×550	W24×55
5	HSS10×10×0.625	W14×193	W14×500	W24×55	HSS10×10×0.625	W14×311	W14×605	W24×55
4	HSS10×10×0.625	W14×145	W14×550	W24×55	HSS10×10×0.625	W14×211	W14×605	W24×55
3	HSS10×10×0.625	W14×99	W14×550	W24×55	HSS10×10×0.625	W14×145	W14×605	W24×55
2	HSS10×10×0.625	W14×48	W14×550	W24×55	HSS10×10×0.625	W14×90	W14×605	W24×55
1	HSS10×10×0.625	-	W14×550	W24×55	HSS10×10×0.625	-	W14×665	W24×55

Table 5 Model 915 and 515 frame sections

| Model ID	915				515			
Story	Brace	Zipper	Column	Beam	Brace	Zipper	Column	Beam
15	W14×730	W14×455	W14×500	W24×55	W14×730	W14×655	W12×96	W24×55
14	HSS7×7×0.500	W14×426	W14×500	W27×539	HSS6×6×0.375	W14×550	W14×605	W27×539
13	HSS7×7×0.500	W14×426	W14×500	W24×55	HSS6×6×0.500	W14×550	W14×605	W24×55
12	HSS7×7×0.500	W14×370	W14×500	W24×55	HSS6×6×0.500	W14×550	W14×605	W24×55
11	HSS8×8×0.500	W14×370	W14×500	W24×55	HSS7×7×0.500	W14×500	W14×605	W24×55
10	HSS8×8×0.500	W14×342	W14×500	W24×55	HSS7×7×0.500	W14×500	W14×605	W24×55
9	HSS8×8×0.500	W14×342	W14×500	W24×55	HSS8×8×0.500	W14×426	W14×605	W24×55
8	HSS8×8×0.625	W14×311	W14×500	W24×55	HSS8×8×0.500	W14×370	W14×605	W24×55
7	HSS8×8×0.625	W14×257	W14×500	W24×55	HSS8×8×0.500	W14×370	W14×605	W24×55
6	HSS8×8×0.625	W14×233	W14×500	W24×55	HSS8×8×0.625	W14×311	W14×665	W24×55
5	HSS8×8×0.625	W14×193	W14×500	W24×55	HSS8×8×0.625	W14×233	W14×665	W24×55
4	HSS10×10×0.625	W14×145	W14×550	W24×55	HSS8×8×0.625	W14×176	W14×665	W24×55
3	HSS10×10×0.625	W14×99	W14×550	W24×55	HSS8×8×0.625	W14×120	W14×665	W24×55
2	HSS10×10×0.625	W14×48	W14×550	W24×55	HSS8×8×0.625	W14×90	W14×665	W24×55
1	HSS10×10×0.625	-	W14×550	W24×55	HSS10×10×0.625	-	W14×665	W24×55
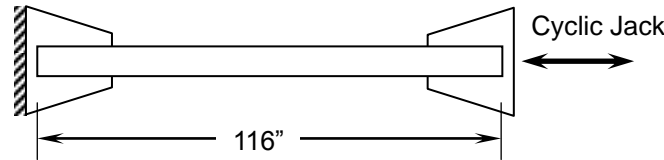
Fig. 8 Geometry of tests specimens in NEES fracture project tube braces

For the purpose of modeling an initial mid span camber with a 1/1000 length for columns and braces was used to model linear and nonlinear buckling. The strain hardening value of 0.003 was used in the modeling. The slope of Coffin-Manson curve in log-log space was set as – 0.485 for hollow square sections and – 0.5 for wide flange sections.

5.1 Brace elements

In this section, 2 specimens tested as the NEES fracture project is modeled, ensuring the accuracy of overall modeling of braces. Fig. 8 shows the geometry of tested specimens.

Fig. 9 shows the load protocol used in testing the specimens, including a far-field and near-field, which induces primarily compression on element.

Figs. 10 and 11 show the modelling results in OpenSEES. Models are constructed using 2 elements and 3 integration points in each one. Using the fiber section, 4 fibers are used in the thickness of each horizontal wall and only one in the width. For the vertical walls of tube, 10 fibers are used in width and 1 in thickness. Corotational geometric transformation is used to construct a

second order analysis as well as adjustment of nodal force direction based on the current element orientation.
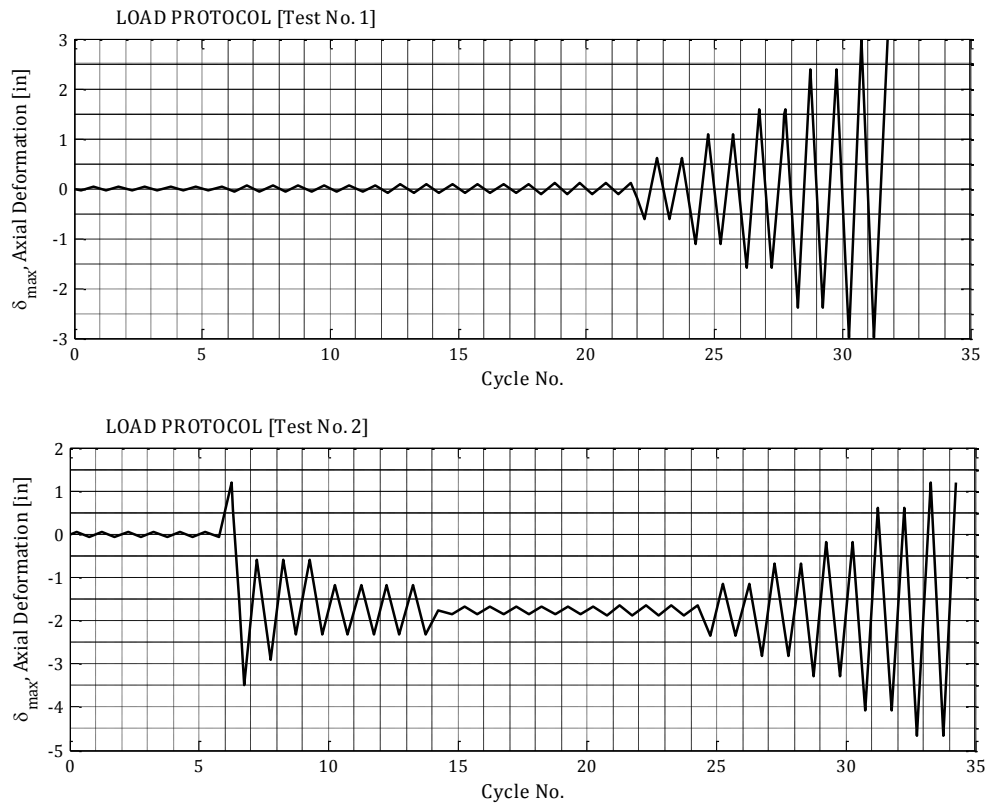

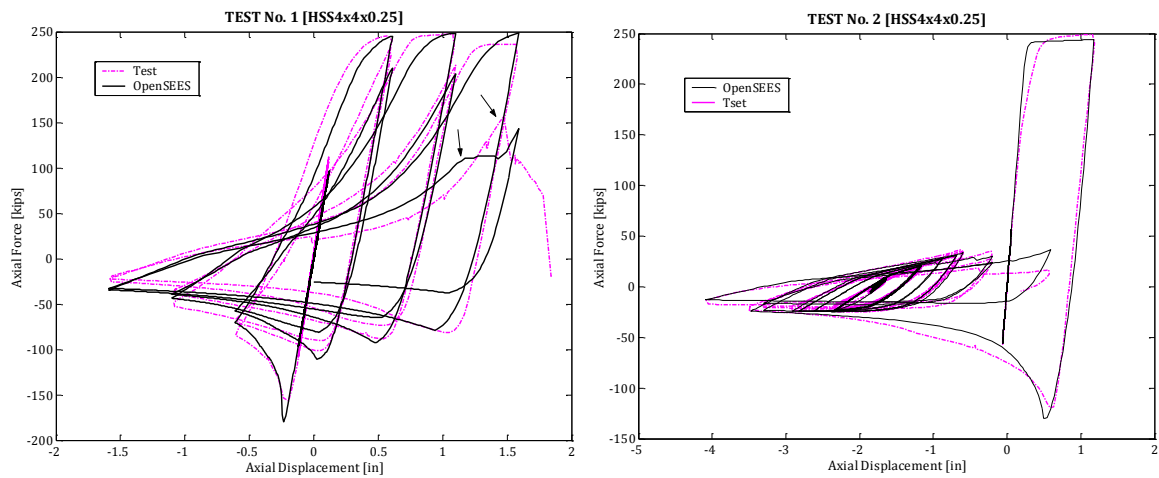Fig. 9 Load protocols of tests specimens in NEES fracture project tube braces

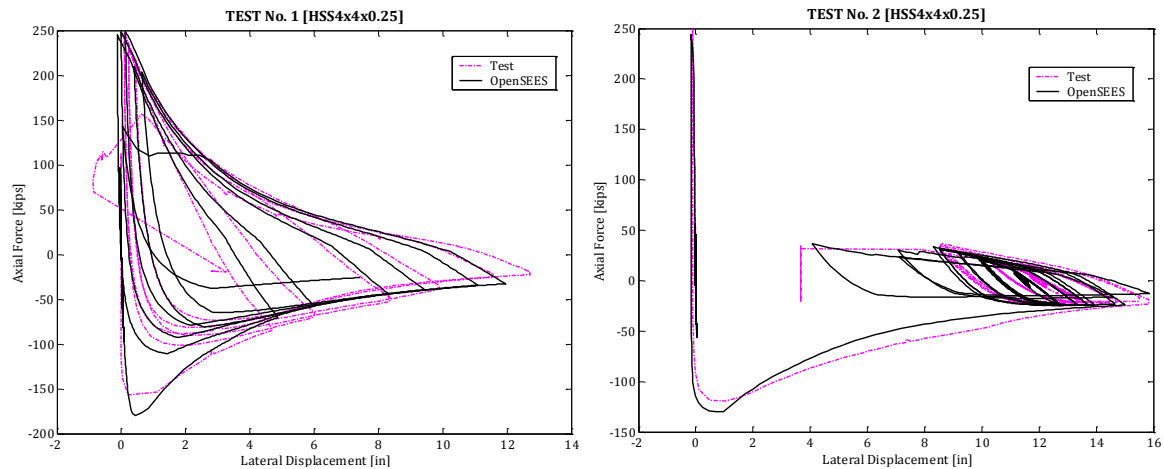Fig. 10 Comparison of test and OpenSEES results for axial force-axial deformation

Fig., 11 Comparison of test and OpenSEES results for axial force-out of plain deformation

5.2 Frames

In this study, two full scale frames were modeled. The first model, Frame-I, is a two story frame (TCBF-HSS-2t) tested at Taiwan in 2008 as part of "International Hybrid Simulation of Tomorrow's Steel Braced Frames" project funded by NEES. The second model, Frame-II, is a two story frame tested at UC-Berkeley (Fell *et al*. 2006).

5.2.1 Frame-I

Tables 6, 7 and 8 illustrate material properties, element cross section and load protocol on the frame, respectively. Fig. 12 shows the frame geometry. Fig. 13 comprise the results of tests undertaken in OpenSEES. The results show that OpenSEES can reasonably predict the cyclic response. While braces buckle, a considerable distance between intersection points of the beam and column and the location of fold lines cause the effective length of brace to be less than what measured between intersection points. This increases frame stiffness and strength.

Table 6 Material Properties used in Modeling of Frame-I

Steel Material Type	BEAM/COL.	BRACE
	A572-Grade 50	A500-Grade B/C
F_y (ksi)	50	46
E (ksi)	29000	29000
R_y (ksi)	not applied	1.4

Table 7 Properties of element section in Frame-I

	Beam (mm)	Column (mm)	Brace (mm)
Flange	PL. 201×19	PL. 307×24	HSS 125×125×9
Web	PL. 506×11	PL. 318×17	

Table 8 Load protocol history applied on Frame-I

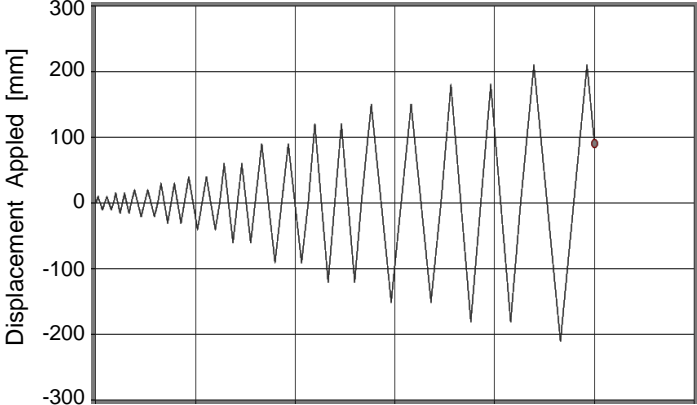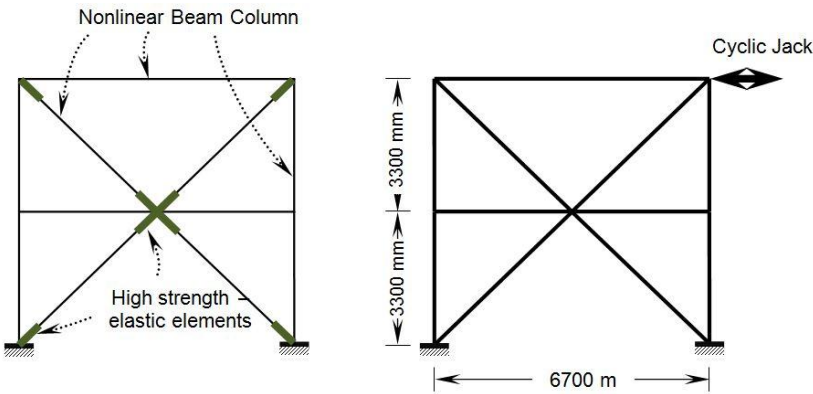| Cycle Num.	δmax (mm)	N
1	10	2
2	15	2
3	20	2
4	30	2
5	40	2
6	60	2
7	90	2
8	120	2
9	150	2
10	180	2
11	210	2

Fig. 12 Geometry of frame-I and elements used to model it in OpenSEES
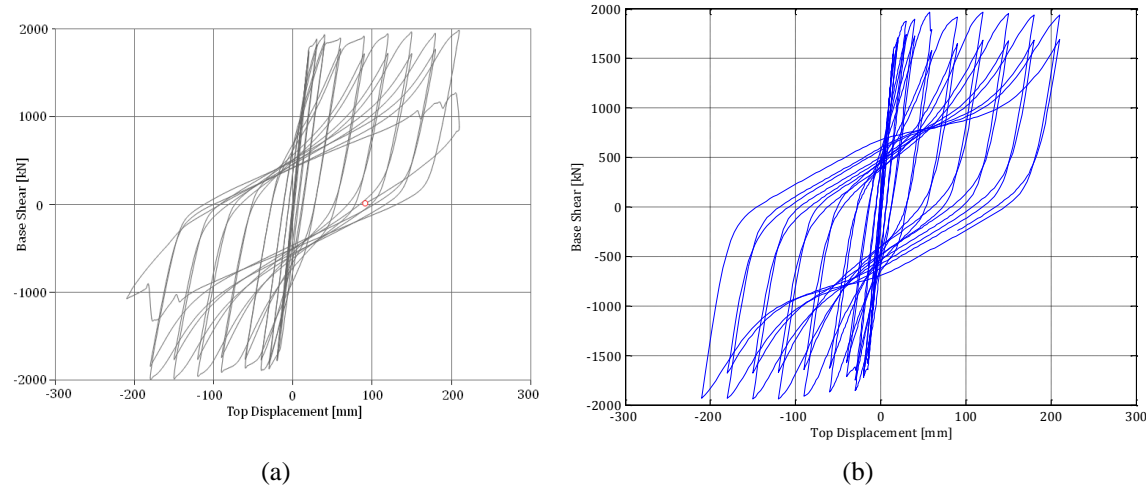

(a) (b)

Fig. 13 Comparison of results of test with OpenSEES. (a) test results, (b) OpenSEES results

5.2.2 Frame-II

This model is selected to examine our ability in modeling of a designed frame. Nonlinearity mainly occurs at the first floor and the second floor remains essentially elastic. Braces are modeled with 20 elements. Tables 9, 10 and 11 illustrate material properties, element cross section and load protocol on the frame, respectively. Fig. 14 shows the frame geometry. Fig. 15 comprises the results of OpenSEES and tests undertaken.

Table 9 Material Properties used in Modeling of Frame-II

Steel Material Type	BEAM	COLUMN	BRACE
	A572-Grade 50	A572-Grade 50	A500-Grade B/C
F_y (ksi)	50	50	46
E (ksi)	29000	29000	29000
R_y (ksi)	1.1	1.1	1.4
$R_y.F_y$	not applied	not applied	64.4

Table 10 Properties of element section in Frame-II

	Beam W24×117	Column W10×45	Brace
Flange	12.8" × 0.85"	8.02" × 0.62"	HSS 6×6×3/8
Web	24.26" × 0.55"	10.10" × 0.35"	

Table 11 Load protocol history applied on Frame-II

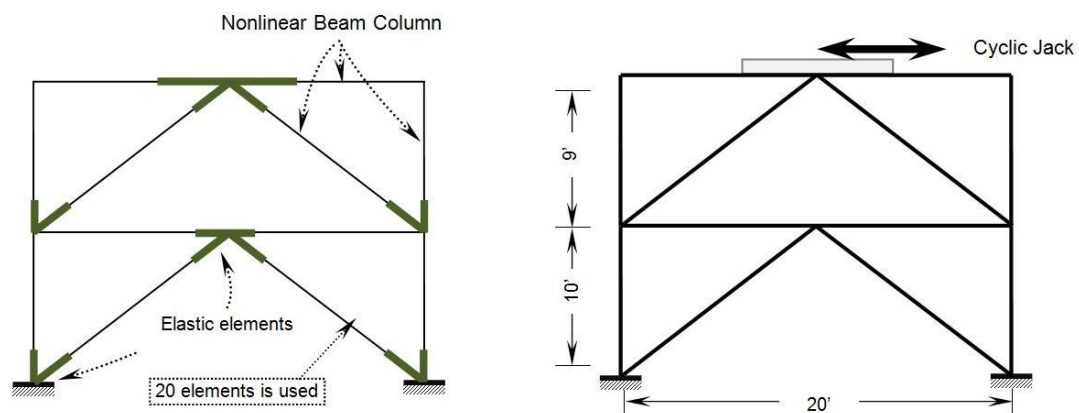| Main Steps	No. of Cycles	Max. displacement at 2nd floor beam
1	6	0.37"
2	4	1.62"
3	4	3.24"
4	2	4.86"

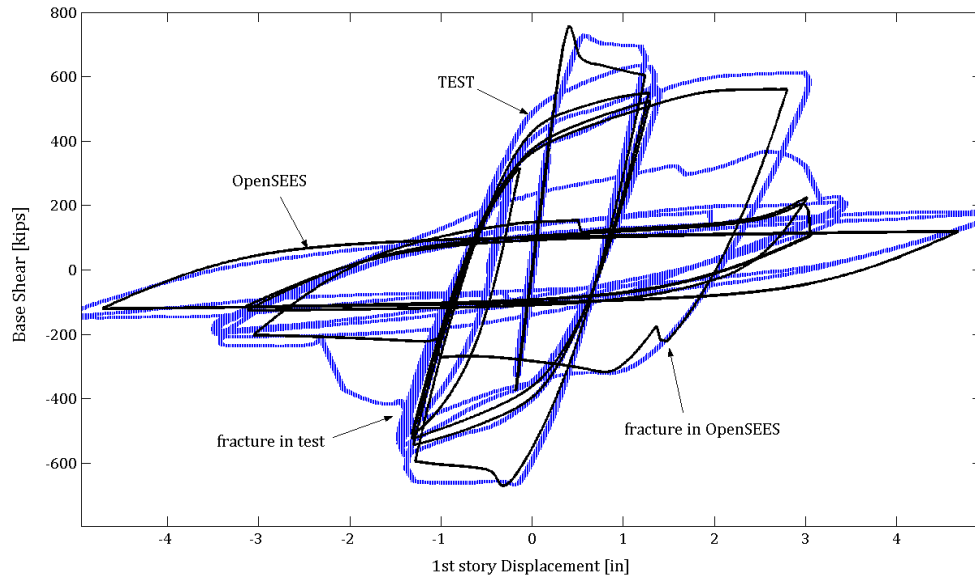Fig. 14 Geometry of frame-I and elements used to model it in OpenSEES

Fig. 15 Comparison the results of test with OpenSEES

6. Response modification factor calculation

6.1 Ground motion sets

Ground motions were selected from the FEMA-P695 (2009) far field records set. The information of records was shown in Table 12. The far field record set includes 22 component pairs of ground motions from sites located at greater than or equal to 10 km from fault rupture with the peak ground acceleration, PGA, greater than 0.2 g and peak ground velocity, PGV, greater than 15 cm/sec and magnitude, *M*, greater than 6.5 (FEMA-P695 2009). Large magnitude events dominate collapse risk and generally have longer duration of shaking, which is important for collapse evaluation of nonlinear degrading models (FEMA-P695 2009).

The primary function of this far field record set is to provide a fully defined set of records for use in a consistent manner to evaluate collapse across all applicable seismic design categories, located in any seismic region, and founded in any soil site classification (FEMA-P695 2009).

6.2 Determining fundamental modes of the models

An eigen value and eigen vector analysis of the models were undertaken to determine the elastic period of the structural models. Determined elastic periods are shown in Table 1.

6.3 Incremental dynamic analysis of the models

For the purpose of the models analyses, a demand measure, DM, and intensity measure, IM, is selected. The DM is inter-story drift ratio in radians and the IM is *Sa(T1)* normalized to gravity acceleration. After normalizing the records for each model, a trial and error procedure was conducted to determine *Sa(T1)* at which the structure collapses. In Fig. 12, an Incremental

Dynamic Analysis (IDA) curve of the models is shown. In the IDA curve, each point corresponds to the result of one nonlinear dynamic analysis of one index archetype model subjected to one ground motion record scaled to one intensity level. The failure criteria or collapse states are defined when one of these conditions is met.

6.3.1 Overriding of maximum allowable inter-story drift

The maximum allowable inter-story drift limit of braced structures is selected from FEMA 356 (2000) which is defined as 2 percents of story height.

6.3.2 Failure Mechanism and structural instability

If the inter-story drift ratio does not exceed the allowable limit, the failure mechanism occurs and the overall system instability will be observed. In this case study, last scaled earthquake data is used. The base shear of the structure under the scaled earthquake in which *Vy* happens is *Ve* (Asgarian and Shogrgozar 2008).

Table 12 Summary information and parameters of selected far field ground motions (FEMA-P695 2009)

ID No.	NEHRP Site Class	Record Seq. No.	Lowest Freq.	Component 1	Component 2	PGA $_{max}$ (g)	PGV $_{max}$ (cm/s)
				File names - Horizontal records			
1	D	953	0.25	NORTHR/MUL009	NORTHR/MUL279	0.52	63
2	D	960	0.13	NORTHR/LOS000	NORTHR/LOS270	0.48	45
3	D	1602	0.06	DUZCE/BOL000	DUZCE/BOL090	0.82	62
4	C	1787	0.04	HECTOR/HEC000	HECTOR/HEC090	0.34	42
5	D	169	0.06	IMPVALL/H-DLT262	IMPVALL/H-DLT352	0.35	33
6	D	174	0.25	IMPVALL/H-E11140	IMPVALL/H-E11230	0.38	42
7	C	1111	0.13	KOBE/NIS000	KOBE/NIS090	0.51	37
8	D	1116	0.13	KOBE/SHI000	KOBE/SHI090	0.24	38
9	D	1158	0.24	KOCAELI/DZC180	KOCAELI/DZC270	0.36	59
10	C	1148	0.09	KOCAELI/ARC000	KOCAELI/ARC090	0.22	40
11	D	900	0.07	LANDERS/YER270	LANDERS/YER360	0.24	52
12	D	848	0.13	LANDERS/CLW-LN	LANDERS/CLW-TR	0.42	42
13	D	752	0.13	LOMAP/CAP000	LOMAP/CAP090	0.53	35
14	D	767	0.13	LOMAP/G03000	LOMAP/G03090	0.56	45
15	C	1633	0.13	MANJIL/ABBAR--L	MANJIL/ABBAR--T	0.51	54
16	D	721	0.13	SUPERST/B-ICC000	SUPERST/B-ICC090	0.36	46
17	D	725	0.25	SUPERST/B-POE270	SUPERST/B-POE360	0.45	36
18	D	829	0.07	CAPEMEND/RIO270	CAPEMEND/RIO360	0.55	44
19	D	1244	0.05	CHICHI/CHY101-E	CHICHI/CHY101-N	0.44	115
20	C	1485	0.05	CHICHI/TCU045-E	CHICHI/TCU045-N	0.51	39
21	D	68	0.25	SFERN/PEL090	SFERN/PEL180	0.21	19
22	C	125	0.13	FRIULI/A-TMZ000	FRIULI/A-TMZ270	0.35	31

6.4 Determining Ve, Vy, Vs and R of models

Ve, *Vy*, *Vs* and *R* used in the models are shown in Table 13. To obtain these values for a suspended zipper braced frame, index archetype models simulated more than 6000 nonlinear dynamic analysis and elastic dynamic analysis. Frames with longer spans in buildings with the same height experience a greater base shear. This is because of the difference in gravity loading. In 9-meter bays, columns are subjected to heavier gravity loads resulting in heavier selected sections for columns and beams in design procedures and it will increase the capacity of the frame to resist lateral loads such as earthquake events.

In Table 14, obtained *R* and its components are shown. As illustrated in Fig. 14, the ductility force reduction factor is almost constant for frames but the over-strength factor differs by stories tall and lateral loading intensity. By increasing the overall height of the building, the over-strength
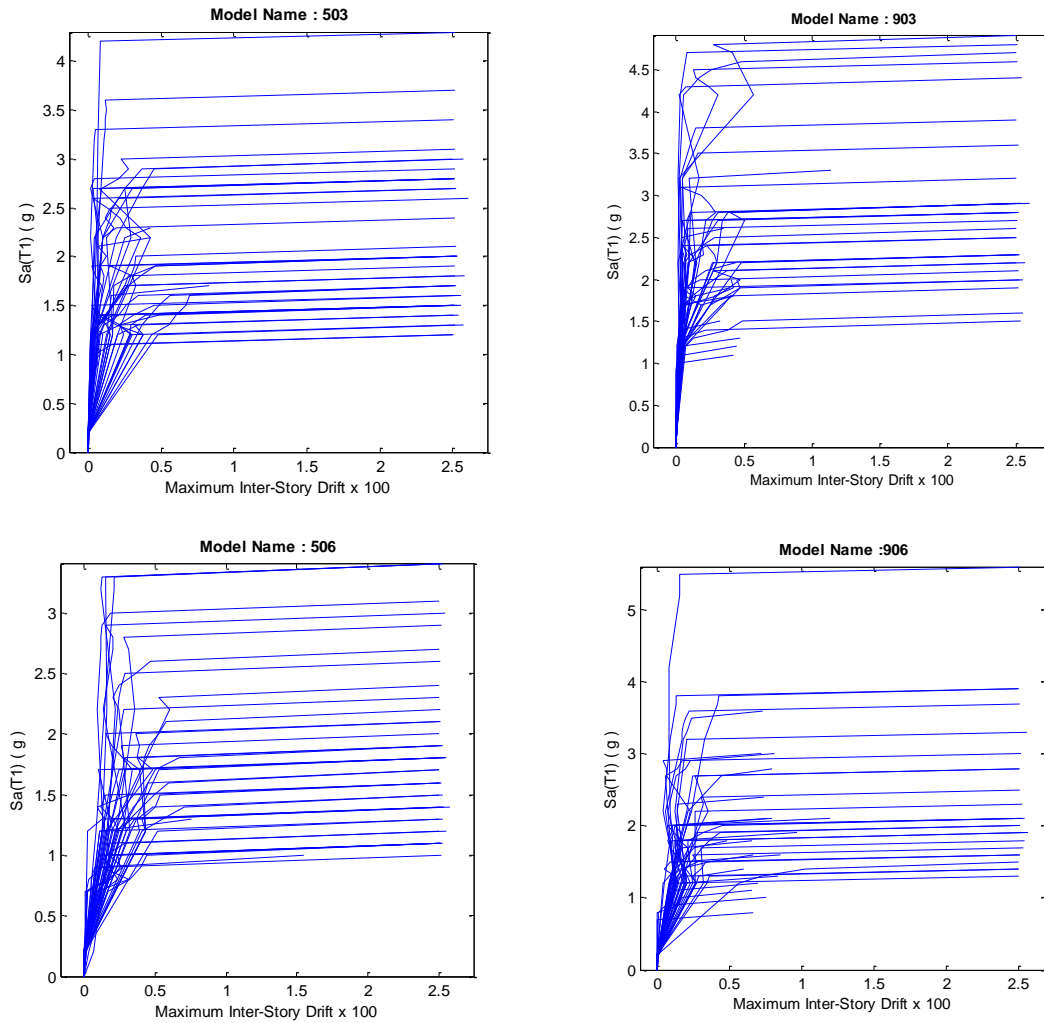

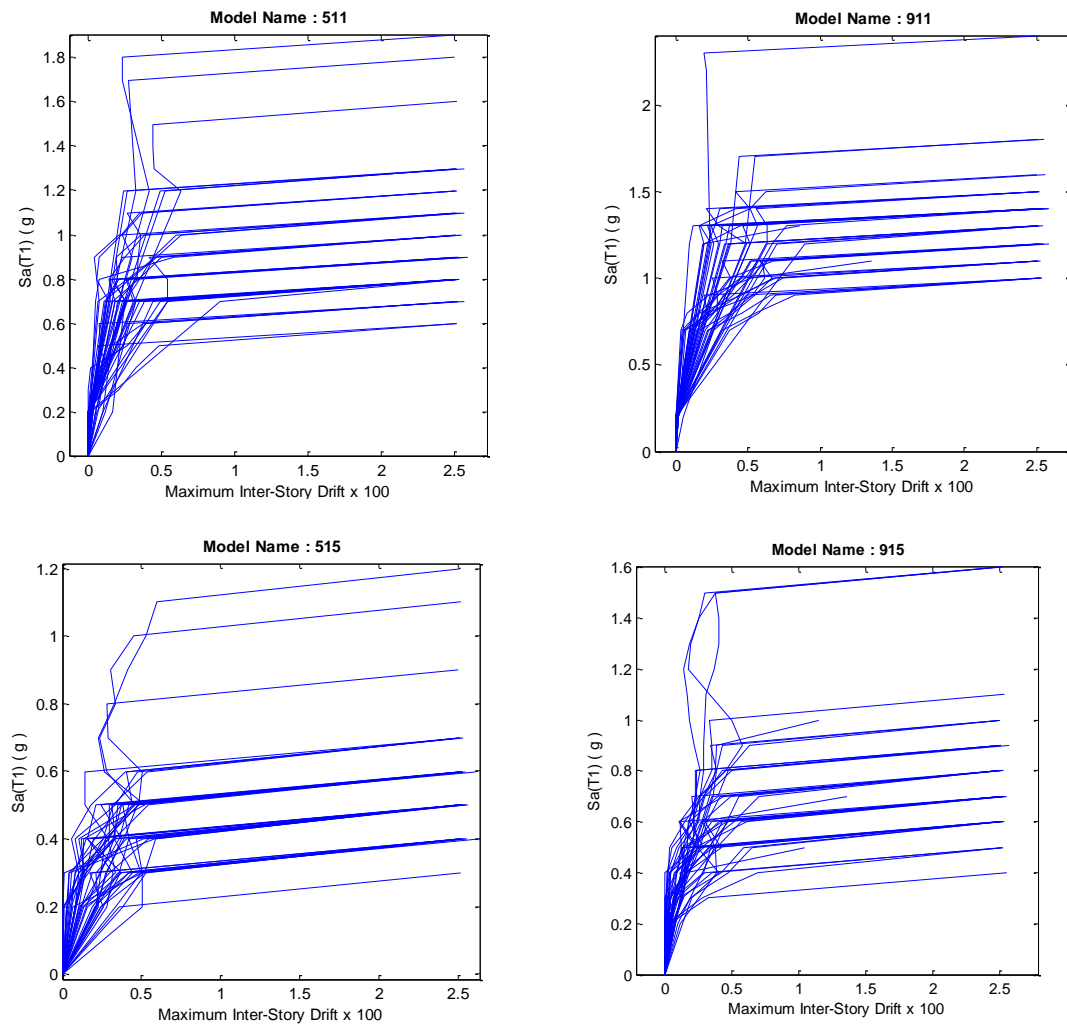Fig. 16 IDA curve of archetype models

Fig. 16 Continued

Table 13 *Ve*, *Vy*, *Vs* of one frame in models

Model ID	*Ve* (KN)	*Vy* (KN)	*Vs* (KN)	*Vs/Vy*	*Ve/Vy*
903	7800.399	4620.3	716.1	0.15	1.69
906	12102.72	7237.7	1432.3	0.20	1.67
911	18000.61	10124	2348.6	0.23	1.78
915	16788.03	9580.1	2059.5	0.21	1.75
503	6506.856	3131.6	716.1	0.23	2.08
506	12027.99	5875.2	1432.3	0.24	2.05
511	16043.84	8186.5	2348.6	0.29	1.96
515	14575.93	7648.2	2059.5	0.27	1.91

factor generally reduces. In Fig. 15 the response modification factor versus the number of stories are plotted. The decreasing pattern changes in the 15-story building because of the change in the lateral load pattern intensity. In 3-,6- and 11-story tall buildings there is 6 lateral load resisting bays in each direction and in 15-story tall buildings, there is 8 lateral load resisting bays. *R* in 9-meter bays are greater than 5-meter ones because of the difference in gravity loadings resulting in heavier sections with more reserve capacity to resist lateral loads.
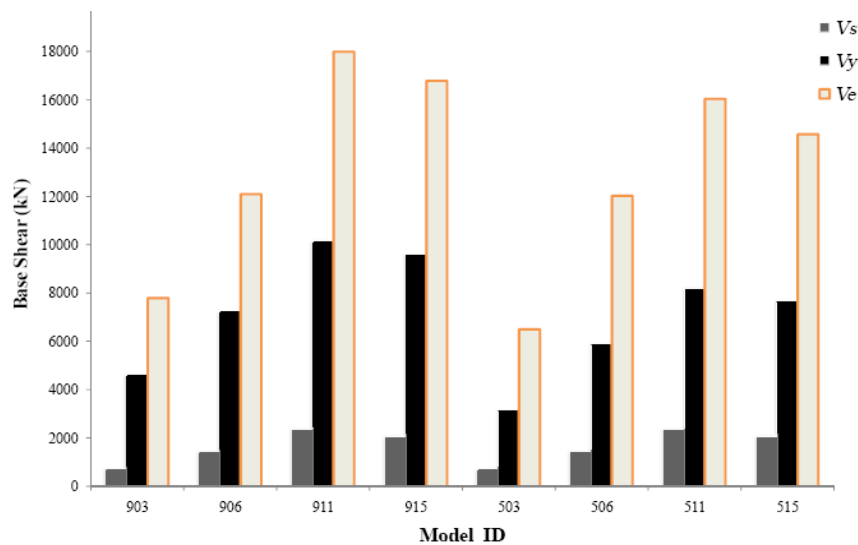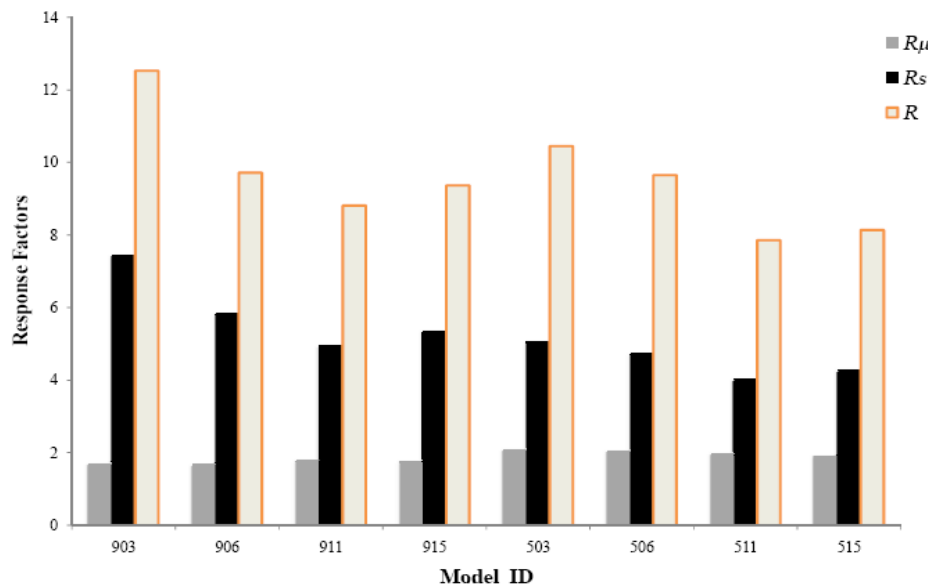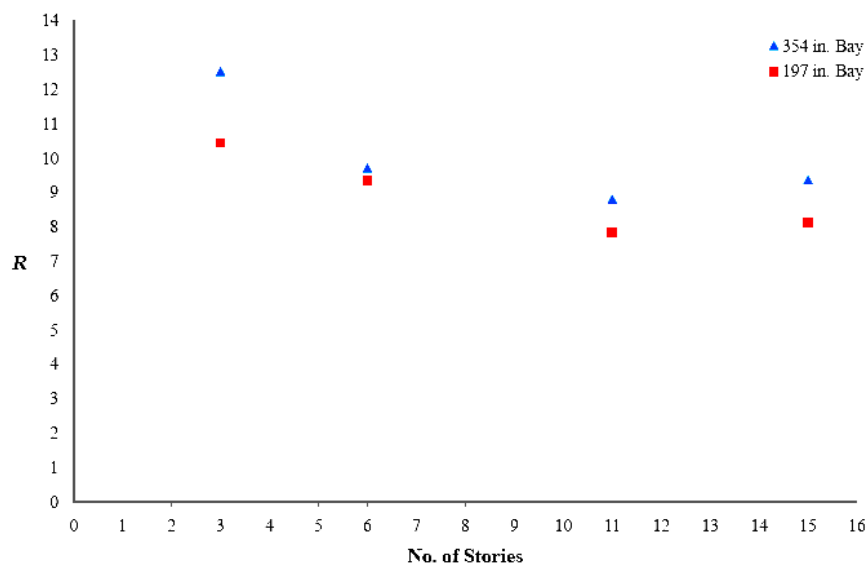

Fig. 17 Base shear of models

Fig. 18 Response modification factor of models

Table 14 Response modification factor of models

Model ID	R_{s0}	R_s	R_μ	R
903	6.45	7.40	1.69	12.52
906	5.05	5.81	1.67	9.71
911	4.31	4.95	1.78	8.81
915	4.65	5.35	1.5	9.37
503	4.37	5.03	2.07	10.45
506	4.10	4.71	2.04	9.65
511	3.48	4.01	1.96	7.85
515	3.71	4.27	1.90	8.14

Fig. 19 Comparison of *R* vs. Number of stories

Geometric mean of response modification factors for suspended zipper frames is determined as 9.5 for the ultimate state approach and 13.6 for the allowable strength approach.

Rs decreases as the height normally increases but in models there is a slight difference in 15-story buildings which is due to a different number of braced spans in them. This indicates that more braced spans outperform heavy section braced spans in lateral excitations.

As the results indicate, *Ve* basically rises by the height increase. However, there is a change in the 15-story buildings because of the number of braced spans. When the number of braced spans increases lateral load will divide into more spans and consequently the sections of braced spans will lighten. It can be deduced that more spans for bracing may cause the structure initial stiffness reduction while more spans increase overall the structure ductility.

7. Conclusions

(1) The response modification factor for suspended zipper frames are proposed as 9.5 and 13.6 for the ultimate limit state design method and allowable stress design method, respectively. These values are larger than the values recommended by AISC (2005) for inverted *V* braced frames.

(2) Different gravity loaded zipper braced frames show different performances implying that in zipper frames, more gravity loading on columns and beams enforces braced frames to use heavier sections. This means these frames have more lateral capacity to resist seismic loads.

(3) The response modification factor of suspended zipper frames decreases as the overall height of the building increases.

(4) More spans for bracing may cause the structure initial stiffness reduction but increases the overall structure ductility which is more desirable.

References

Abdollahzadeh, G.R. and Banihashemi, M. (2013), "Response modification factor of dual moment-resistant frame with buckling restrained brace (BRB)", *Steel Compos. Struct., Int. J.*, **14**(6), 621-636.

AISC (2005), Seismic Provisions for Structural Steel Buildings, American Institute of Steel Construction, Chicago, IL, USA.

ASCE (2005), Minimum Design Loads for Buildings and Other Structures, American Society of Civil Engineers.

Asgarian, B. and Shokrgozar, H.R. (2008), "BRBF response modification factor", *J. Construct. Steel Res.*, **65**(2), 290-298.

ATC-19 (1995), Structural response modification factors, Applied Technology Council, Redwood City, CA, USA.

ATC-34 (1995), A critical review of current approaches to earthquake resistant design, Applied Technology Council, Redwood City, CA, USA.

Bruneau, M., Uang, C.M. and Wittaker, A. (1998), *Ductile Design of Steel Structures*, McGraw-Hill, New York, NY, USA.

Fell, B.V., Kanvinde, A., Deierlein, G., Myers, A. and Fu, X. (2006), "Buckling and Fracture of Concentic Braces Under Inelastic Cyclic Loading", Steel Technical Information and Product Services (SteelTIPS), Moraga, CA, USA.

FEMA-P695 (2009), Quantification of Building Seismic Performance Factors, Federal Emergency Management Agency, Washington, D.C., USA.

FEMA 356 (2000), Seismic Rehabilitation Pre-Standard, Federal Emergency Management Agency, Washington, D.C., USA.

Goel, S.C. (1992), "Earthquake resistant design of ductile braced steel structures", Stability and Ductility of Steel Structures under Cyclic Loading, CRC Press, Boca Raton, FL, USA.

Khatib, I.F., Mahin, S.A. and Piester, K.S. (1988), "Seismic behavior of concentrically braced steel frames", Earthquake Engineering Research Center, UCB/EERC-88/01.

Kim, J., Cho, C., Lee, K. and Lee, C. (2008), "Design of zipper column in inverted *V* braced steel frames", *Proceedings of the 14th World Conference on Earthquake Engineering*, Beijing, China, October.

Leon, T.R. and Yang, C.S. (2003), "Special inverted V braced frames with suspended zipper struts", National Center for Research on Earthquake Engineering, International Workshop on Steel and Concrete Composite Construction, IWSCCC, Taipei, Taiwan.

Mazzolani, F.M. and Piluso, V. (1996), Theory and Design of Seismic Resistant Steel Frames, E & FN Spon, London, UK.

Mozzoni, S., McKenna, F., Scott, M.H., Fenves, G.L. and Jeremic, B. (2004), OpenSEES command

language manual.

Mwafi, A.M. and Elnashi, A.S. (2002), "Calibration of force reduction factors of RC buildings", *Journal of Earthquake Engineering*, **6**(22): 239-73.

Han, S.W., Kim, W.T. and Foutch, D.A. (2007), "Tensile strength equation for HSS bracing members having slotted end connections", *Earthq. Eng. Struct. Dyn.*, **36**(8), 995-1008.

Kim, J., Cho, C., Lee, K. and Lee, C. (2008), "Design of zipper column in inverted *V* braced steel frames", *Proceedings of the 14th World Conference on Earthquake Engineering*, Beijing, China, October.

Schmidt, B.J. and Barlett, F.M. (2002), "Review of resistance factor for steel: Resistance distributions and resistance factor calibration", *Can. J. Civil Eng.*, **29**(1), 109-118.

Tremblay, R. and Trica, L. (2003), "Behavior and design of multi-story zipper concentrically braced steel frames for the mitigation of soft-story response", *Proceedings of the 13ᵗʰ World Conference on Earthquake Engineering*, Vancouver, BC, Canada, August.

Uang, C.M. (1991), "Establishing *R* (or Rw) and Cd factor for building seismic provision", *J. Struct. Eng.*, **117**(1), 19-28.

Uriz, P. (2005), "Toward earthquake-resistant design of concentrically braced steel-frame structures", Ph.D. Thesis, University of California at Berkeley, Berkeley, CA, USA.

Uriz, P. and Mahin, S.A. (2004), "Seismic vulnerability assessment of concentically braced frames", *J. Steel Struct.*, **4**, 239-248.

Yang, C.S. and Leon, R. (2003), "Special inverted V braced frames with suspended zipper struts", Doctoral Dissertation, Georgia Institute of Technology, GA, USA.

Yang, C., Leon, R. and DesRoches, R. (2010), "Cyclic behavior of zipper-braced frames", *Earthq. Spectra*, **26**(2), 561-582.

CC